

P012

## Exploration of the Deep Structure of the Central Greece Geothermal Field by Passive Seismic and Curie Depth Analysis

V.K. Karastathis\* (National Observatory of Athens), J. Papoulia (Hellenic Centre for Marine Research), B. Di Fiore (National Observatory of Athens), J. Makris (GeoPro GmbH), A. Tsambas (Hellenic Centre for Marine Research), A. Stampolidis (Aristotle University of Thessaloniki) & G.A. Papadopoulos (National Observatory of Athens)

### SUMMARY

---

New findings about the deep origin of the geothermal fields and volcanic centres of the North Evian Gulf area, Central Greece, were arisen by combining a three-dimensional travelttime inversion study of a microseismic dataset recorded of 37 portable stations together with a Curie depth point analysis based on aeromagnetic data.

A possible magma chamber can be presumed by the detection of a low seismic velocity volume with high Poisson ratio values at depths below 8 km and the Curie point depth estimation at about 7-8 km depth as well.

Besides, the analysis gave information about how the main large tectonic structures (NW-SE) and other important NE-SW faults can facilitate the hydrothermal flux of the local geothermal field.

## Introduction

Along the coast of the North Evian Gulf, Central Greece, there are significant geothermal sites and thermal springs as Aedipsos, Yaltra, Lichades, Iliia, Kamena Vourla, Thermopylae etc. (Figure 1) but also volcanoes of the Quaternary - Pleistocene age as Lichades and Vromolimni. Since for these local volcanoes and geothermal fields, their deep origin and their relation with the ones of the wider region (Thessaly or Central Evia, see Figure 1) have not been clarified yet in detail, we attempted a deep structure investigation by conducting a 3D local earthquake tomography study in combination with Curie Depth analysis of aeromagnetic data. The study area is shown in the map of Figure 1.

A combined onshore - offshore network of 23 stand alone stations and 7 Ocean Bottom Seismographs (OBS's) was deployed to record the microseismic activity for a 4-month period, in the summer of 2003. The locations of the land seismographs and OBSs as well as the epicentres of the 2000 recorded events, as these were initially located by Papoulia et al. (2006), are presented in Figure 2a.

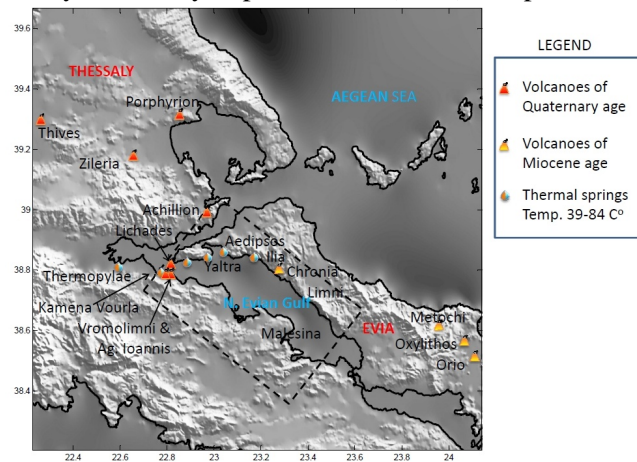


**Figure 1** Map of the Central-East Greece presenting the volcanic centres and the sites of the most important thermal springs. The dashed line box indicates the study area.

## Methodology and Data processing

### a. *Traveltime inversion of microseismicity data*

To build the 3D seismic velocity structure we implemented the algorithm SIMULPS14 (Thurber, 1983; Eberhart-Phillips, 1990; Haslinger and Kissling, 2001). The code performs simultaneous inversion of the model parameters  $V_p$ ,  $V_p/V_s$  and hypocenter locations. It uses a linearised damped least-square inversion to solve the non-linear problem of the hypocentral location and velocity model. The parameterisation of the velocity model is accomplished by the considering a 3D grid of velocity nodes ( $V_p$  and  $V_p/V_s$ ) with linear interpolation of the velocity values in the intermediate space.

Due to the non-linear nature of the problem, the initial velocity model and hypocenter locations in the inversion procedure must be chosen as close as possible to their true values. A good approximation can be derived by adopting the "1-D minimum velocity model" resulting from the VELEST algorithm (Kissling et al., 1994). In order to build a reliable minimum 1D velocity model we used only the most reliable events depending on the number of phases. We set a minimum of 8 records per event and azimuthal gap (GAP) be lower than  $180^\circ$  ( $GAP < 180^\circ$ ) and selected 481 events. The initial  $V_p/V_s$  values were chosen close to 1.78 based on previous studies in the wider region. The VELEST algorithm simultaneously inverted the hypocentral parameters and the velocity model to obtain the optimum solutions (1D minimum model). The initial and final model of the 1D inversion is presented in Figure 2b with the black and red line respectively. For the design of the input model for VELEST we took into account the results of a past seismic survey (Makris et al., 2001). The 3D linearised tomography code SIMULPS14 was afterwards applied to determine the 3D velocity structure of the P

and S waves. The initially recorded seismicity (Papoulia et al., 2006) was then relocated using the final 3D velocity model.

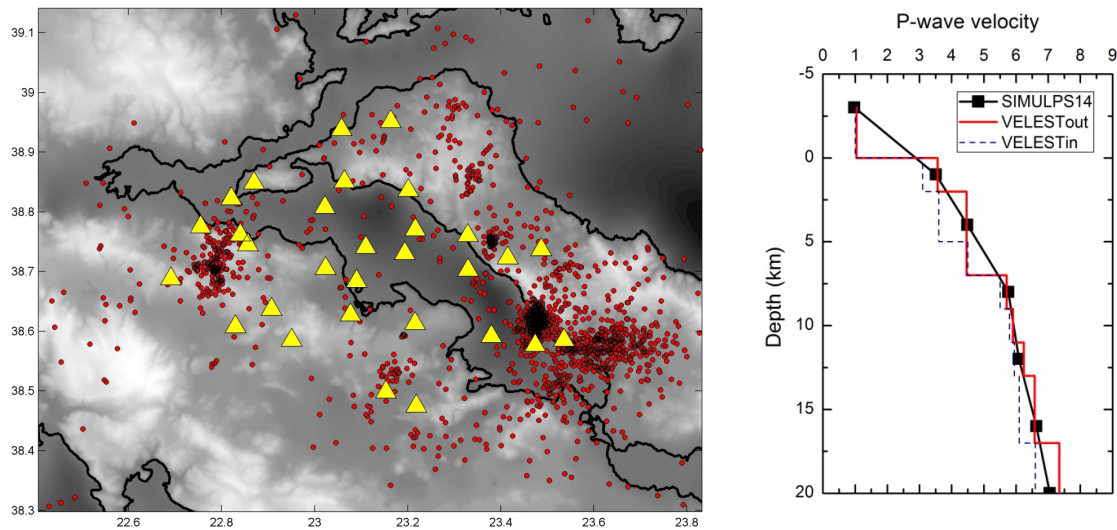


**Figure 2** Location map of the seismograph stations and the initial epicentres (Papoulia et al. 2006) (left). The input (VELESTin) and final (VELESTout) 1D model of Velest algorithm. The input model was based on geophysical results (Makris et al. 2001). The input model for the 3-D inversion (SIMULPS14) was based on the VELEST output (right).

The three-dimensional inversion required as basic inputs the initial velocity model, the travetime P-wave and S-wave phases of the recorded microseismicity and the stations characteristics. The number of the events increased in this procedure to 540 with the selection of the ones with minimum number of P-wave phases equal to 6. In the selection criteria was also the azimuthal gap (GAP) to be lower than  $180^\circ$ . The values of the damping factors were chosen with the aid of the trade-off curve between the model variance and data variance. Two horizontal slices of the 3D P-wave velocity model and the respective ones of the Poisson ratio are given in Figure 3(a, b, c, d). The dashed lines in Figures 3 imply the reliability limit that we finally considered based on the comparison between the graphical representations of the diagonal elements of the resolution matrix (RDE) and the recovery ability of “checkerboard” models (Figures 3e, 3f).

### **b. Curie Point Depth estimation by aeromagnetic data**

To estimate the Curie Depth Point we followed the centroid procedures described in Stampolidis et al., (2005). The filtered residual dataset of the area was subdivided in 5 square sub-regions, C1 to C5, sized  $100 \times 100 \text{ km}^2$  with a 70% overlap. In each sub-region the radially averaged power spectra were computed using the Philips (1997) software. The slope of the longest wavelength part for each sub-region yielded the centroid depth,  $z_o$ , of the deepest layer of magnetic sources, while the slope of the second longest wavelength spectral segment yielded the depth to the top,  $z_t$ , for the same layer (an example, the C1 square area, is reported in Figure 4). Using the formula  $z_b = 2z_o - z_t$  (Okubo et al. 1985) the Curie Depth estimation was derived for each sub-region C an assigned at its centre. The estimated depths are reported in km below sea level (Figure 4).

### **Interpretation of the results**

The most important structural feature detected by the three-dimensional local earthquake tomography was a low velocity anomaly (relative to the initial 1D reference model) below the region of North Evian gulf at depths of 8-12 km and deeper. The negative velocity anomaly is obvious in both sections of 8 and 12 km depth (Figure 3). The resolution at the 16 km depth slice does not allow us to have a clear picture on how this anomaly continues deeper. However, the good resolution part of the

section shows that such a continuation is possible. The anomaly zone also presents high values of Poisson ratio, in the order of 0.28 or higher to 0.32 (eg. Aediposos-Ilia at 8 km, Vromolimni at 12 km).

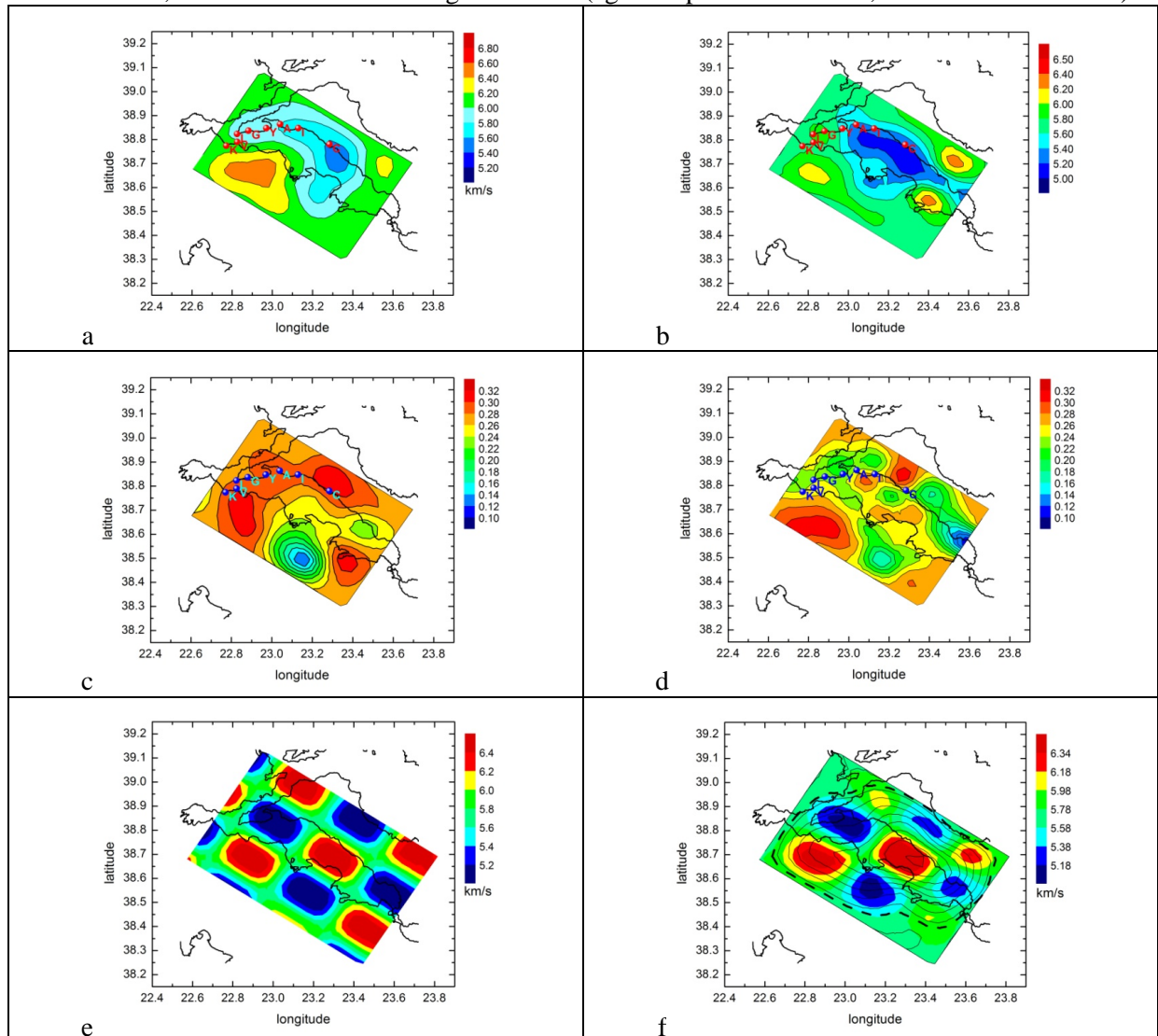


**Figure 3** Horizontal slice of the P-wave velocity for the depths of 12 km (a) and 8 km (b) and the respective slices of Poisson ratio (c) and (d). The detected anomaly is correlated also with the position of the local volcanic and geothermal centres, namely K: Kamena Vourla V: Vromolimni L: Lichades G: Agios Georgios Port of Lichades Y: Yaltra A: Aediposos I: Ilia C: Chronia. At the bottom figures the checkerboard test is presented; the model used to produce the synthetic data (e) and the resulted model after the inversion procedure with 1D starting model.

Since high temperature magmatic chambers are characterized by low seismic velocities, high Poisson ratios and elevated Curie surfaces, we could identify that a possible magmatic chamber is located in an approximate depth of 8 to 12 km and possibly deeper. Present day hydrothermal activity is supporting this assumption.

The existence of the higher velocity material at 8 km below Lichades and Vromolimni implies a possible presence of crystallized magma.

The seismic slices of 4 km depth showed that the thermal springs follow existing active faults.

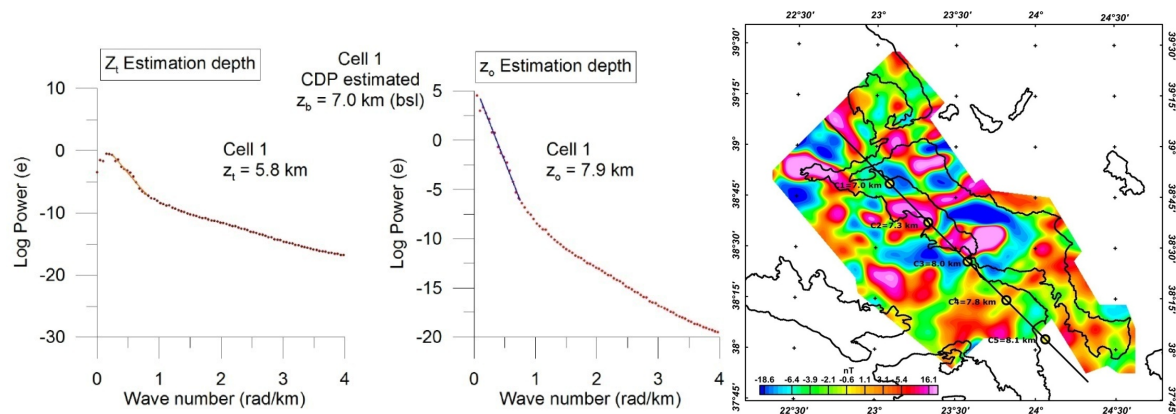


**Figure 4** Example of CDP estimated depths for Cell 1 over band-pass filtered (10-50 km) data set (left). Aeromagnetic map of the wider region. The estimated CDP depths have been also depicted in their positions (right)

## Conclusions

The joint study of seismic velocity tomography from local earthquake observations and the Curie Depth Point analysis from aeromagnetic data provided a reliable approximation of the depth and thermal properties of intruded high temperature sources below North Evoikos gulf geothermal field. Depth of these sources was deduced from low velocity P and S values and high Poisson ratios at about 8 – 12 km depth and deeper. Since the Curie Depth Point analysis estimated the demagnetization of the material due to high temperatures at the top of this volume, we concluded that this volume is related with the existence of a magma chamber. Below the Quaternary volcanoes of Lichades, Vromolimni and Agios Ioannis there is a local increase of the seismic velocity over the low velocity anomaly. This was attributed to a crystallized magma volume below the volcanoes. The coincidence of the spatial distribution of surface geothermal sites and volcanoes with the deep low velocity anomaly supports our consideration of magma presence.

## Acknowledgments

We would like to thank Dr S. Husen (Swiss Seismological Service, ETH) for the technical discussions about the tomography method we had. We thank as well, the scientists of IGME, Mr G. Hatziyannis, Dr T. Kavouridis, Mr P. Vakalopoulos, Mr Gr. Vrellis and Dr P. Giannouloupoulos and also Dr I. Gerolymatos (EYDAP) and S. Liakopoulos for the discussions we had about the geothermal field of the study area. We are finally grateful to Dr Karmis (IGME) who provided us part of the aeromagnetic data and the GSRT for financing the project “Amphitrite”.

## References

- Haslinger, F. and Kissling, E. [2001] Investigating effects of 3-D ray tracing methods in local earthquake tomography. *Physics of the Earth and Planetary Interiors*, **123**, 103–114.
- Kissling E. [1995] *Veltest user's guide*. Internal report. Institute of Geophysics, ETH Zurich, pp 26
- Makris, J., Papoulia, J., Papanikolaou, D., Stavrakakis, G. [2001] Thinned continental crust below northern Evoikos Gulf, central Greece, detected from deep seismic soundings. *Tectonophysics*, **341**, 225–236.
- Okubo, Y., Graf, R.J., Hansen, R.O., Ogawa, K., Tsu, H. [1985]. Curie point depths of the island of Kyushu and surrounding areas. Japan. *Geophysics*, **50**, 481-494.
- Papoulia, J., Makris, J., Drakopoulou, V. [2006] Local seismic array observations at north Evoikos, central Greece, delineate crustal deformation between the North Aegean Trough and Corinthiakos Rift. *Tectonophysics* **423**, 97–106.
- Phillips, J.D. [1997] *Potential-Field Geophysical Software for the PC, version 2.2*. Open-File Report, U.S. Geological Survey, 97-725.
- Stampolidis, A., Kane I., Tsokas G.N., Tsourlos P. [2005]. Curie point depths of Albania inferred from ground total field magnetic data. *Surveys in Geophysics*, **26**, 461-480.
- Thurber, C.H. [1983]. Earthquake locations and three dimensional crustal velocity structure in the Coyote lake area, central California. *Journal of Geophysical Research*, **88**, 8226–8236.